This item is likely protected under Title 17 of the U.S. Copyright Law. Unless on a Creative Commons license, for uses protected by Copyright Law, contact the copyright holder or the author.

Access to this work was provided by the University of Maryland, Baltimore County (UMBC) ScholarWorks@UMBC digital repository on the Maryland Shared Open Access (MD-SOAR) platform.

Please provide feedback

Please support the ScholarWorks@UMBC repository by emailing scholarworks-group@umbc.edu and telling us what having access to this work means to you and why it's important to you. Thank you.

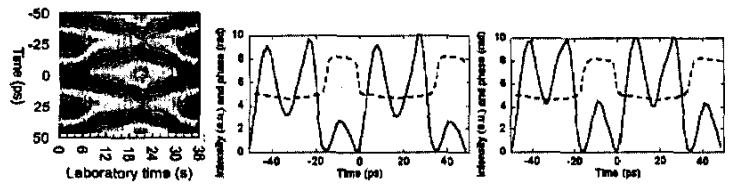

Fig. 4. Intensity plot of the temporal intensity of the pulse as a function of the laboratory time (left, high values of the intensity are in white and low values are in black). Around t=0 s and t=36 s, 33 % RZ pulses are obtained, while around t=12 s and 26 s, 67 % CSRZ pulses are obtained, as in Fig. 2. The middle and right plots are two pulse shapes measured at a 1 second interval around t=5 s.

operation. The master clock at 10 GHz is doubled and split into two 20 GHz sine waves which are amplified and sent to the two driving ports of the modulator. Depending on the bias, a 33 % RZ (Return-to-Zero) or 67 % CSRZ (Carrier-Suppressed Return-to-Zero) train of pulses can be obtained. Proper carving requires the adjustment of the amplitudes of the two sine waves, of their relative phase and of the bias. The high update rate of our diagnostic allowed real-time optimization of the bias for the proper settings for 33 % RZ or 67% CSRZ. The accuracy of the new fast implementation is tested against the previous implementation of spectrograms, which is based on an Ando AQ6317 to measure the spectra of the gated pulses. As in [1], a 64 by 64 trace is constructed and inverted, and the complete retrieval of the field takes about 3 minutes. The comparison of the measured electric fields with the two techniques is displayed in Figure 2 for 33 % RZ and 67 % CSRZ pulses. An excellent agreement is obtained, even though the fast implementation is about 1000 times faster than the slow one. Note the perfect retrieval of the phase jump between adjacent pulses in the case of 67% CSRZ pulses.

2. Comparison with a fast sampling scope
The temporal intensity retrieved by the fast spectrogram was compared to the waveform measured by a Newport 40 GHz detector and a Tektronix 50-GHz sampling scope. The measured intensities are plotted in Figure 3 in the case of when the bias is set to get 33 % RZ pulses and when the bias is set arbitrarily. The limited bandwidth of the high-speed sampling scope is clearly apparent on these plots.

3. Real-time optimization of pulse carving
The fast implementation of the spectrogram technique was used to provide a real-time accurate measurement of the pulse shape in order to optimize the pulse carver. The very high bandwidth of this tool provides a unique ability to measure small imperfections of the pulse shape, and therefore track overdriving, underdriving, or improper value of the bias of the Mach-Zehnder modulator. The bias of the modulator was changed continuously and the carved waveform evolved continuously from 33 % RZ carving (Fig. 2, left) to 67 % CSRZ (Fig. 2, right), then to some arbitrary waveform and then back to 33 % RZ carving in 36 seconds, a time that corresponds to 320 measurements. The temporal intensity that is measured by our device as a function of time is plotted on an intensity plot in Figure 4. Two pulse shapes measured at a 1 second interval are also plotted. This demonstrates the sensitivity of our pulse characterization device to small changes in the pulse shape, as well as the potential for real-time optimization or feedback using such a diagnostic.

5. Conclusions
The real-time characterization of optical pulses using spectrograms has been demonstrated. Such a diagnostic provides the complete measurement of the electric field of a periodic train of pulses, with a great bandwidth improvement over fast electronic sampling scopes. With an update rate close to 10 Hz, this diagnostic can be used for real-time monitoring and optimization of the electric field. The use of a scanning etalon as a frequency-resolving device also allows easy integration.

[1] J. Debeau, B. Kowalski and R. Boittin, "Simple method for the complete characterization of an optical pulse." Opt. Lett., **23**, 1784-1786 (1998).
[2] L. P. Barry, S. Del Burgo, B. Thomsen, R. T. Watts, D. A. Reid and J. Harvey, "Optimization of optical data transmitters for 40-Gb/s lightwave systems using frequency resolved optical gating." IEEE Photon. Technol. Lett., **14**, 971-973 (2002).
[3] C. Dorrer and I. Kang, "Simultaneous characterization of telecommunication optical pulses and modulators." Opt. Lett., **27**, 1315-1317 (2002).
[4] D. Kane, "Recent progress toward real-time measurement of ultrashort laser pulses." IEEE J. Quant. Electron., **35**, 421-431 (1999).

MF81 **5:30 PM**

Computation of the Q-Factor in Optical Fiber Systems Using an Accurate Receiver Model

I. T. Lima, Jr., A. O. Lima, J. Zweck, C. R. Menyuk,
University of Maryland Baltimore County,
Baltimore, MD, Email: lima@engr.umbc.edu.

We derive an analytical expression that explicitly relates the Q-factor to the optical signal-to-noise ratio in optical fiber transmission systems with any given pulse shape and receiver characteristics using an accurate receiver model.

1. Introduction
A fundamental problem in the design of optical fiber transmission systems is to achieve a desired bit-error rate (BER) after the signal is transmitted through a single channel or a wavelength-division multiplexed (WDM) system. Since direct BER measurements can be difficult to obtain, a widely used performance measure is the Q-factor, which can be used to give an approximate value for the BER under the assumption that the electrical currents in the marks and in the spaces at the receiver are Gaussian distributed. The Q-factor is a function of the means and the variances of the currents in the marks and in the spaces that are obtained experimentally in the time domain using an oscilloscope. The optical signal-to-noise ratio (OSNR) is another commonly used indicator of performance that is even easier to measure than the Q-factor [1]. However, the relationship between the OSNR and the Q-factor is not straightforward, since it depends on the characteristics of the receiver and on the shape of the optical pulses after transmission.
The design and performance evaluation of optical fiber communication systems relies just as much on the accuracy and efficiency of receiver models as it does on accurate and efficient modeling of the transmission line [2]. Accurate receiver modeling is especially important for format comparison studies. Marcuse [3] derived an approximate expression for the Q-factor as a function of the signal-to-noise ratio (SNR) of the electrical current in a nonreturn-to-zero (NRZ) system with an optically preamplified receiver that consists of a rectangular optical filter, a square-law detector, and an integrate-and-dump electrical filter. In this letter, we generalize Marcuse's result by deriving an analytical formula for the Q-factor in terms of the OSNR for an arbitrary optical pulse shape immediately prior to the receiver and for arbitrary optical and electrical filters in the receiver. In order to correctly account for the pulse shape in this formula we define an enhancement factor, which explicitly quantifies how efficiently the combination of a pulse shape and a receiver translates the OSNR into the SNR of the electrical current in the receiver.

2. Theory
In this section we derive an expression that relates the Q-factor to the OSNR. We begin by recalling the analytical expressions for the mean and the variance of the electrically filtered current in the receiver as in [2]. At the receiver, we assume that noise from the optical amplifiers is the dominant source of noise, as is the case in an optically preamplified receiver [4]. At the input to the receiver, we assume that the signal is polarized and we let $e_{in}(t)$ denote its scalar-valued electric field, where t is time. We also assume that the noise is unpolarized white Gaussian noise that has been generated by optical amplifiers. More specifically, let

$$n_{\parallel s}(t) \text{ and } n_{\perp s}(t)$$

be the components of the noise whose polarization states are, respectively, parallel and perpendicular to the polarization state of the signal. These two orthogonal components of the noise are delta-correlated with mean zero and constant power spectral density per polarization N_{ASE} over the optical spectrum of a channel. Our receiver model consists of an optical filter

$$H_o(\omega)$$

with impulse response $h_o(t)$, a square-law photodetector, and an electrical filter

$$H_e(\omega)$$

with impulse response $h_e(t)$. Then the current at the receiver is given by
(1)

$$i(t) = R\left\{\left|\left[e_{in}(t) + n_{\parallel s}(t)\right] * h_o(t)\right|^2 + \left|n_{\perp s}(t) * h_o(t)\right|^2\right\} * h_e(t),$$

where R is the responsivity of the photodetector and the convolution of two functions $g(t)$ and $h(t)$ is defined by .

$$g(t) * h(t) = \int_{-\infty}^{+\infty} g(\tau)h(t-\tau)d\tau$$

From Eq. (1), the mean current due to noise is given by

$$\langle i_n\rangle(t) = \langle i_n\rangle = 2N_{ASE}RB_o, \text{ where } \langle\cdot\rangle(t)$$

is the average over the statistical realizations of the noise at time τ, and

$$B_o = \int_{-\infty}^{+\infty} |h_o(\tau)|^2 d\tau$$

is the power-equivalent spectral width [5] of the optical filter. The mean current due to noise is time-independent since the optical noise is a stationary random process. The variance of the current at any time τ is given by
(2)

$$\sigma_i^2(t) = \langle i^2\rangle(t) - \langle i\rangle^2(t) = \sigma^2_{ASE-ASE} + \sigma^2_{S-ASE}(t).$$

The first term on the right of Eq. (2), which is the variance of the current due to noise-noise beating in the receiver, is given by
(3)

$$\sigma^2_{S\text{-}ASE}(t) = 2N_{ASE}R^2\mathrm{F}_t^{-1}\left\{H_e\mathrm{F}_\tau\left[e_{out}(\tau)\mathrm{F}_\tau^{-1}\left\{\left|\tilde{H}_o\right|^2\mathrm{F}_{\tau'}\left[e^*_{out}(\tau')h_e(t-\tau')\right]\right\}\right]\right\}$$

where

$$\tilde{H}_o(\omega) = H_o(-\omega),$$

Authorized licensed use limited to: University of Maryland Baltimore Cty. Downloaded on June 06,2025 at 16:07:23 UTC from IEEE Xplore. Restrictions apply.

while $\mathcal{F}_\tau[\cdot]$ and $\mathcal{F}_\tau^{-1}\{\cdot\}$ indicate the Fourier transform with respect to τ and its inverse. The second term, which is the variance of the current due to signal-noise beating in the receiver, is given by
(4)

$$_{SE}(t) = 2R^2 N_{ASE} \mathcal{F}_t^{-1}\left\{H_s \mathcal{F}_\tau\left[e_{out}(\tau)\mathcal{F}_\tau^{-1}\left\{\left|\tilde{H}_o\right|^2 \mathcal{F}_{\tau'}\left[e_{out}^*(\tau')\, h_s(t-\tau')\right]\right\}\right]\right\},$$

where

$$e_{out}(t) = e_{in}(t) * h_o(t)$$

is the optically filtered electric field of the signal.

We now use these analytical results to derive a general expression for the Q-factor as a function of the OSNR following a procedure similar to the one described in [3], but using the true mean and the true variance of the electrical current. In this derivation we assume that the extinction ratio of the electrical current in the receiver is so small that the variance of the current in the spaces is dominated by the noise-noise beating [4]. We start with the standard time-domain definition of the Q-factor,

$$Q = (\langle i_1\rangle - \langle i_0\rangle)/(\sigma_1 + \sigma_0)$$

as in [3], which is related to the BER by

$$\mathrm{BER} = \mathrm{erfc}\left(Q/\sqrt{2}\right)/2 \approx \exp(-Q^2/2)/\left(Q\sqrt{2\pi}\right)$$

provided that the electrical currents in the marks and in the spaces are Gaussian-distributed. We define the OSNR by

$$\mathrm{OSNR} = \langle |e_{in}(t)|^2\rangle_t / (2N_{ASE} B_{OSA}), \text{ where } \langle |e_{in}(t)|^2\rangle_t$$

is the time-averaged noiseless optical power per channel prior to the optical filter, and B_{OSA} is the power-equivalent spectral width of an optical spectrum analyzer (OSA) that is used to measure the optical power of the noise. We find that for any optically preamplified amplitude-shift-keyed system with perfect extinction ratio the Q-factor can be expressed as a function of the OSNR as
(5)

$$Q = \frac{\xi\,\mathrm{OSNR}}{1+\sqrt{K\xi\,\mathrm{OSNR}+1}}\sqrt{M},$$

where ξ is the enhancement factor, K is the signal-noise beating parameter and M is the effective number of noise modes, all of which are unitless. The parameters
(6)

$$M = \frac{\langle i_n\rangle^2}{\sigma^2_{ASE-ASE}} \quad \text{and} \quad K = \frac{\langle i_n\rangle\,\sigma^2_{S-ASE}(t_1)}{i_{1s}\sigma^2_{ASE-ASE}}$$

are determined by the shapes of the receiver filters and K also depends on the shape of the optical pulse immediately prior to the receiver. In the equation for K, the time t_1 at which the the variance of the current due to signal-noise beating is evaluated corresponds to the sampling time of a mark. The enhancement factor ξ is the ratio between the signal-to-noise ratio, SNR, of the electrical current of the marks and the OSNR at the receiver, and can be expressed as
(7)

$$\xi = \frac{\mathrm{SNR}}{\mathrm{OSNR}} = \frac{i_{1s}}{\langle i_n\rangle}\frac{2N_{ASE}B_{OSA}}{\left\langle |e_{in}(t)|^2\right\rangle_t} = \xi'\frac{B_{OSA}}{B_o},$$

where i_{1s} is the noiseless current of the marks at the clock recovery time. The normalized enhancement factor

$$\xi' = i_{1s}/(R < |e_{in}(t)|^2 >_t)$$

quantifies how efficiently the combination of the pulse shape and receiver translates the OSNR into the SNR of the electrical current in the receiver. All three parameters,

ξ, K, and M, should be taken into account in the optimization of the receiver performance. Equation (5) can easily be generalized for systems with arbitrary extinction ratio.

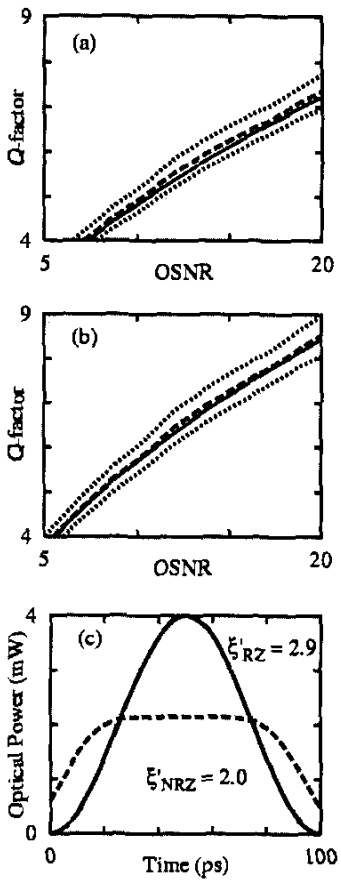

Fig. 1: Comparison between the analytical and the time domain Monte Carlo methods of computing the Q-factor as a function of the OSNR. (a) Results for the NRZ format shown in Fig 1.c. The solid line shows the Q-factor computed using the analytical method. The dashed line and the two dotted lines show the mean Q-factor and the confidence interval, defined by the mean Q-factor plus and minus one standard deviation, respectively, computed using the time domain Monte Carlo method. (b) The same as in Fig. 1.a for the RZ raised cosine format shown in Fig. 1.c. (c) A comparison of the optical pulse shapes together with their normalized enhancement factors. The solid curve shows the shape of the RZ raised cosine pulse and the dashed curve shows the shape of an isolated mark in the NRZ format.

3. Numerical Results

We now validate the analytical method for computing the Q-factor from the OSNR by comparison with Monte Carlo simulations in which the Q-factor is computed from the equation

$$Q = (\langle i_1\rangle - \langle i_0\rangle)/(\sigma_1 + \sigma_0)$$

We validate the method using two back-to-back 10 Gbit/s optical fiber transmission systems with optical noise added by a Gaussian noise source with constant spectral density within the spectrum of the optical filter. In Fig. 1.a we plot the Q-factor versus the OSNR for an NRZ pulse shape with a rise time of 30 ps, and in Fig. 1.b we show the corresponding result for a return-to-zero (RZ) raised cosine format with a 50% duty cycle. The receiver consisted of a Gaussian-shaped optical filter with a full-width at half maximum of 62 GHz and a fifth-order low-pass electrical Bessel filter with a 3 dB-width of 7 GHz. The power-equivalent spectral width of the OSA is equal to 25 GHz. The results for the analytical method, that we show with solid lines, were obtained using only a single mark and a single space of the transmitted bit string. The results for the time-domain Monte Carlo method that we show with dashed lines were obtained by averaging over 100 samples of Q, where for each sample the means and standard deviations of the marks and spaces were estimated using 256 bits. The agreement between the two methods is excellent. We used a perfect extinction ratio for these simulations. In Fig. 1.c we compare the NRZ and RZ raised cosine optical pulse shapes used for the results in Figs. 1.a and 1.b. For the NRZ format the parameters in Eqs. (5)-(7) are

$\xi = 0.8$

$\xi = 2.0$

and $K=2.9$, while for the RZ format

$\xi' = 1.0$

$\xi' = 2.9$

and $K=3.1$. The parameter M is equal to 13 in both systems. For the results shown in Figs. 1.a and 1.b, and also for those in Ref. [2], the primary reason the RZ format has a better back-to-back performance than the NRZ format is that it has a larger normalized enhancement factor ξ. In [1] and [3], $K=2$, since the electrical filter was approximated by an integrate and dump filter. For these receivers, the use of this approximation overestimates the Q-factor by up to 25%.

4. Conclusions

In conclusion, we have derived an accurate formula that relates the Q-factor to the OSNR for amplitude-shift-keyed optical fiber transmission systems with arbitrary optical pulse shapes and receiver characteristics using a realistic receiver model. This method can be used in receiver optimization studies, and it can also be applied to the study of other amplitude-shift-keyed formats. Since the method is computationally efficient, it can be used for the analysis of transmission systems that have pattern dependences due to effects such as chromatic and polarization-mode dispersion and the Kerr nonlinearity. We validated this method by comparison with Monte Carlo simulations.

References:

1. E. Golovchenko, *Tutorial OFC 2002*, TuL.
2. P. Winzer, *et al.*, *JLT.*, **19**, No. 9, 2001.
3. D. Marcuse, *JLT.*, **8**, No. 12, 1990.
4. L. Kazovsky, *et al.*, *Optical Fiber Communication Systems*, Artech House, 1996.
5. B. Saleh, *et al.*, Fundamentals of Photonics, John Wiley & Sons, 1991.

MF82 **5:30 PM**

Effects of Partially Polarized Noise in a Receiver

Y. Sun, I. Lima, A. Lima, H. Jiao, J. Zweck, L. Yan, C. Menyuk, G. Carter, *University of Maryland Baltimore County, Baltimore, MD;* G. Carter, *The Laboratory for Physical Sciences, College Park, MD, Email: yusun@umbc.edu.*

We compare back-to-back experiments to an accurate receiver model and an analytical formula

Authorized licensed use limited to: University of Maryland Baltimore Cty. Downloaded on June 06,2025 at 16:07:23 UTC from IEEE Xplore. Restrictions apply.